

Tomohiro Namimoto
Yasuyuki Yamashita
Kazuo Awai
Takeshi Nakaura
Yumi Yanaga
Toshinori Hirai
Tetsuo Saito
Hidetaka Katabuchi

Combined use of T2-weighted and diffusion-weighted 3-T MR imaging for differentiating uterine sarcomas from benign leiomyomas

Received: 20 December 2008
Revised: 28 March 2009
Accepted: 25 April 2009
Published online: 6 June 2009
© European Society of Radiology 2009

H. Katabuchi
Obstetrics and Gynecology,
Graduate School of Medical Sciences,
Kumamoto University,
1-1-1, Honjo,
Kumamoto, 860-8556, Japan

Abstract The objective of our study was to compare diffusion-weighted imaging (DWI) alone and DWI combined with T2-weighted MRI for the differentiation of uterine sarcomas from benign leiomyomas. T2-weighted imaging and DWI were performed in 103 patients with 103 myometrial tumours, including 8 uterine sarcomas and 95 benign leiomyomas on 3-T MR imaging. The signal intensity (SI) of the tumour on T2-weighted images was quantified as the tumour-myometrium contrast ratio (TCR) by using the following formula: $(SI_{\text{tumour}} - SI_{\text{myometrium}}) / SI_{\text{myometrium}}$. The TCR or apparent diffusion coefficient (ADC) value alone and then the ADC value combined with T2-weighted imaging were evaluated for differentiation between

sarcomas and leiomyomas. The mean ADC value of sarcomas was $0.86 \pm 0.11 \times 10^{-3} \text{ m}^2/\text{s}$, which was significantly lower than that of leiomyomas $1.18 \pm 0.24 \times 10^{-3} \text{ m}^2/\text{s}$; however, there was a substantial overlap. The mean TCR of sarcomas was 0.66 ± 0.71 , which was significantly higher than that of the leiomyomas, -0.37 ± 0.34 ; however, again, there was a considerable overlap. When ADC was less than $1.05 \times 10^{-3} \text{ mm}^2/\text{s}$ and TCR was greater than 0 this condition was considered to confirm a sarcoma; a combination of ADC and TCR achieved a significant improvement without any overlap between sarcomas and leiomyomas (sensitivity 100%, specificity 100%). Our preliminary results indicate that combined DWI and T2-weighted MR imaging is better than DWI alone in the differentiation of uterine sarcomas from benign leiomyomas.

Keywords Diffusion · ADC · Magnetic resonance imaging · uterus · sarcoma

T. Namimoto (✉) · Y. Yamashita ·
K. Awai · T. Nakaura · Y. Yanaga ·
T. Hirai
Department of Diagnostic Radiology,
Graduate School of Medical Sciences,
Kumamoto University,
1-1-1, Honjo,
Kumamoto, 860-8556, Japan
e-mail: namimotoo@yahoo.co.jp
Tel.: +81-96-3735261
Fax: +81-96-3624330

T. Saito
Radiation Oncology,
Graduate School of Medical Sciences,
Kumamoto University,
1-1-1, Honjo,
Kumamoto, 860-8556, Japan

Introduction

Uterine sarcomas are one of the most difficult neoplasms to cure in gynaecological oncology. Their malignant behaviours such as rapid growth and high rate of metastasis are notorious. Uterine sarcomas are often difficult to differentiate from leiomyomas, which is the most common

tumour of the uterine myometrium. Recently, uterus-preserving treatments, such as gonadotropin-releasing hormone analogues [1], uterine arterial embolisation [2] and focused ultrasound surgery [3], have been widely indicated for leiomyomas. Therefore, pretreatment imaging diagnosis of the uterine sarcomas has become important. As an endometrial biopsy may not usually be helpful for

the definitive diagnosis of uterine sarcomas, magnetic resonance (MR) imaging may play an important role in diagnosing these tumours and determining appropriate management. On MR imaging, uterine sarcomas often manifest as a large infiltrating myometrial mass of intermediate to high signal intensity on T2-weighted images [4–9]. On the other hand, common benign leiomyomas often manifest as low signal intensity on T2-weighted images. Therefore, MR imaging usually allows specific diagnosis of common benign leiomyomas [10, 11]. However, leiomyomas may occasionally be associated with various types of degeneration or cellular histologic subtype, which can cause increased signal intensity on T2-weighted images [1, 12]. In such instances, the differentiation between benign and malignant myometrial tumours may be difficult if only based on the signal intensity of conventional non-enhanced and post-contrast MR sequences.

Diffusion-weighted imaging (DWI) is a recently developed technique used to show tissue characteristics based on the diffusion motion of water molecules. Although DWI now plays an important role in the diagnosis of brain disorders [13–15], it has not been fully applied in body imaging as the image quality suffers from blurring because of the long readout interval and from artefacts caused by high susceptibility to resonance offsets. In addition, various artefacts caused by bowel motion and air in the intestine were found to degrade image quality. Recent advances in MR technology such as higher magnetic field strengths, parallel imaging techniques [16] and phased-array receiver coils have finally made the acquisition of DWI in the body feasible for clinical use by decreasing the distortion and imaging time. One of the greatest advantages of DWI in the abdomen is that this technique can delineate malignant lesions as a hyperintense area with excellent tissue contrast [17–20]. DWI can also provide quantitative measurement of apparent diffusion coefficient (ADC) values, which are considered to be influenced by the nuclear-to-cytoplasm ratio and cellular density in solid tissues [13, 22–24]. Decreased ADC values of malignant tumours compared with normal tissues or benign lesions have been previously reported for various organs [17–21, 25]. In the female pelvis, the utility of DWI for ovary, uterine cervical and endometrial cancers has been previously reported [26–29]. Some investigators have attempted ADC measurement of benign leiomyomas [30–32]. However, only one study reported that the utility of DWI for uterine sarcomas plays a limited role because of a large overlap between sarcomas and benign leiomyomas [33]. On the other hand, to our knowledge, the utility of DWI for the female pelvis on a 3-T MR unit has not previously been investigated.

The purpose of this study was to compare DWI alone and DWI combined with T2-weighted imaging for the differentiation of uterine sarcomas from benign leiomyomas on 3-T MR imaging.

Materials and methods

Study population

Our study was approved by our institutional review board, which waived the requirement for informed patient consent. The study population included 103 consecutive women, aged 24–78 years (mean age 47.8 years), who underwent MR examination with DWI for various uterine myometrial masses at our institution from January 2007 to May 2008. Eight uterine sarcomas were confirmed in eight patients by surgery. Histopathological diagnoses for these eight uterine sarcomas consisted of leiomyosarcomas ($n=4$), endometrial stromal sarcomas ($n=2$) and mixed mesodermal tumours ($n=2$). Thirty-five of 95 cases of uterine leiomyomas were confirmed by surgery. Another sixty cases of leiomyomas were diagnosed by MR imaging with negative cytology of endometrial mucosa, and 6-month follow-up MR imaging or ultrasonography (US) was performed (mean follow-up 324 days). Leiomyomas were defined as nodules delineated from adjacent tissues by sharp margins in T2-weighted images by two experienced radiologists (To.N., Ta.N., with 15 and 10 years of experience, respectively, including subspecialty training in body imaging) in consensus [11]. Sixty-eight women were premenopausal (66%) and 35 postmenopausal (34%). Exclusion criteria for this study included patients with leiomyomas smaller than 2 cm in diameter and patients with only adenomyosis, although patients with concomitant leiomyoma and adenomyosis were included in this study. In patients with multiple leiomyomas, only the largest tumour was included for the image analysis. The diameter of myometrial tumours measured on MR images ranged from 2.1 to 21.3 cm (mean 5.8 ± 3.3 cm).

MR imaging protocol

All MR examinations were performed with a 3-T superconductive MR unit (Acheiva 3 T; Philips Medical Systems, Best, Netherlands) using a six-channel SENSE torso coil. Spin-echo T1-weighted images (TR/TE=590/10 ms, flip angle 90° , 2 excitations) in the axial plane and turbo-spin-echo (TSE) T2-weighted images (TR/TE=4,000/100 ms, flip angle 90° , 17 echo train length, 2 excitations) in the sagittal and axial planes with a parallel imaging technique (SENSE factor of 2) were acquired. Spin-echo T1-weighted images and TSE T2-weighted images were obtained with a section thickness of 5 mm, an intersection gap of 1 mm, matrix of 512×512 and field of view (FOV) of 250 mm. In 46 patients, including all sarcoma patients, sagittal and axial contrast-enhanced T1-weighted images were additionally obtained after the acquisition of DWI. Dynamic contrast-enhanced MR imaging was performed with all sarcomas and 22 leiomyomas. DWI was obtained in the axial plane with a

section thickness of 6 mm, an intersection gap of 1 mm and FOV of 300 mm using a single-shot echo-planar imaging sequence (TR/TE=3,100/53 ms, flip angle 90°, 2 excitations, matrix of 256×256) with the chemical shift selective (CHESS) fat suppression technique and a parallel imaging technique (SENSE factor of 2). The corresponding b values to the diffusion-sensitising gradient were 0 and 1,000 s/mm². ADC maps were derived automatically on a pixel-by-pixel basis from the DWI according to the following equation:

$$ADC = -[\ln(S1) - \ln(S0)] / (b1 - b0),$$

where b_0 and b_1 represent b values of lower and higher values, respectively, and S_0 and S_1 are the signal intensities (SI) for these b values.

Image analysis

MR images were retrospectively evaluated in consensus by two experienced radiologists (To.N., Ta.N., with 15 and 10 years of experience respectively, including subspecialty training in body imaging), who were blinded to the diagnostic results. MR images were reviewed regarding the following items: size of the tumour (the greatest diameter), SI of the lesion and myometrium on T2-weighted imaging and DWI. We defined a new parameter for evaluating the SI of the tumour on T2-weighted imaging, the tumour-myometrium contrast ratio (TCR). The TCR between the lesion and myometrium in the uterus was quantified on T2-weighted imaging by using the following formula:

$$(SI_{\text{tumour}} - SI_{\text{myometrium}}) / SI_{\text{myometrium}}, \text{ where } SI_{\text{myometrium}}$$

is the average of the regions of interest (ROI) of the myometrium SI, SI_{tumour} is the average ROI of the tumour SI on T2-weighted images. The circular ROI of the myometrium was placed to be as large as possible beside the mass, excluding the junctional zone. The TCR value was positive when the ROI of the tumour had higher SI than the outer myometrium. The TCR value was negative when the ROI of the tumour had lower SI than the outer myometrium.

As for quantitative analysis, one of the readers (To.N.) recorded the ADC values of each tumour by placing the ROI on ADC maps on a clinical viewer (Yokogawa Medical Systems). The circular ROI was placed to be as large as possible within the confines of the tumour, without involving artefacts from tumour/air interface or blood flow. For heterogeneous lesions, special attention was paid not to involve necrosis or cystic space within the lesion by referring to T1- and T2-weighted images and contrast-enhanced T1-weighted images. The ADC values of the normal myometrium were also measured in the same way. The TCR of the tumour and normal myometrium was also

measured in the same ROI. For comparison of the results, differences between the normal myometrium, leiomyomas and uterine sarcomas with respect to the ADC values and TCR were assessed using the unpaired t test followed by Tukey's multiple comparison test. Differences with $p < 0.05$ were considered statistically significant.

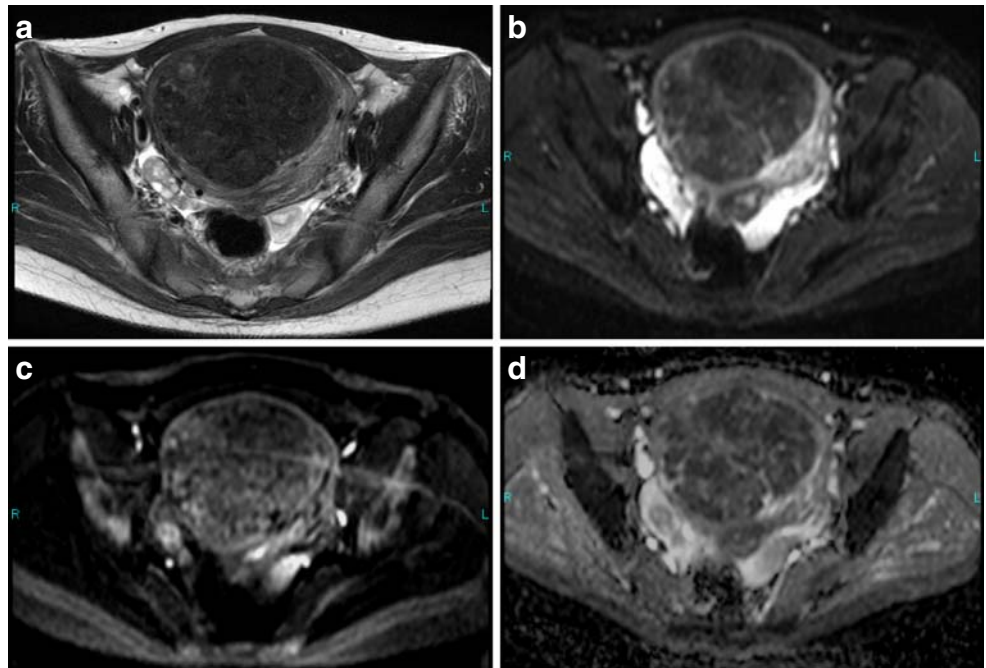
Results

The ADC values of myometrial tumours and the outer myometrium were successfully measured in all subjects. The mean and the standard deviation of the ADC value of the normal myometrium ($n=103$), leiomyomas ($n=95$) (Figs. 1 and 2) and uterine sarcomas ($n=8$) (Figs. 3, 4 and 5) were 1.54 ± 0.22 , 1.18 ± 0.24 and 0.86 ± 0.11 ($\times 10^{-3}$ mm²/s), respectively. The ADC values of uterine sarcomas and leiomyomas were significantly lower ($p < 0.01$) than those of the normal myometrium. The mean ADC value of sarcomas was significantly lower ($p < 0.01$) than that of leiomyomas (Fig. 6). However, the ADC values overlapped substantially for uterine sarcomas and leiomyomas. The mean and the standard deviation TCR of sarcomas were 0.66 ± 0.71 , which was significantly higher ($p < 0.01$) than that of the leiomyomas -0.37 ± 0.34 (Fig. 7); however, there was a considerable overlap. Figure 8 shows scatter plots of TCR versus ADC values of leiomyomas and uterine sarcomas. When ADC was less than 1.05×10^{-3} mm²/s and TCR was greater than 0 this condition was considered to indicate a sarcoma; a combination of ADC and TCR was achieved without any overlap between sarcomas and leiomyomas (sensitivity 100%, specificity 100%) (Fig. 8). The combination of ADC and TCR is significantly better than the ADC value or TCR alone ($p < 0.01$).

Discussion

In the present study, all uterine sarcomas showed high SI on DWI. The mean ADC value of sarcomas was lower than that of the normal myometrium, which corresponds to the previously published literature reporting on decreased ADC values in various malignant tumours [17–20]. The decrease in ADC values in malignant tissue is attributed to histopathological characteristics, including hypercellularity, enlargement of nuclei, hyperchromatisms and angulation of the nuclear contour, that result in a reduction of diffusional displacement of water molecules [13, 22–24]. In this study, we have shown that T2-weighted images combined with DWI were able to differentiate between uterine sarcomas and leiomyomas without any overlap. Tamai et al. [33] reported that the mean ADC value ($\times 10^{-3}$ mm²/s) of sarcomas was 1.17 ± 0.15 , which was lower than those of the normal myometrium (1.62 ± 0.11) and degenerated leiomyomas (1.70 ± 0.11), without any overlap; however, they did overlap with those of ordinary leiomyomas and cellular

Fig. 1 A 31-year-old woman with ordinary leiomyoma of the myometrium. **a** Axial T2-weighted image shows a leiomyoma of distinct low intensity in the myometrium. The TCR between the mass and the myometrium is -0.74 . **b** DWI on b_0 shows the mass as an area of homogeneous hypointensity. **c** DWI on $b_{1,000}$ visualises mass as an area of hypointensity. When DWI on b_0 and $b_{1,000}$ are compared, a slight signal loss is detected on $b_{1,000}$ images. **d** ADC map demonstrates the tumour as an area of hypointensity relative to the normal myometrium caused by the “T2 blackout effect”. The ADC values of leiomyoma and the normal myometrium are $0.99 \times 10^{-3} \text{ mm}^2/\text{s}$ and $1.66 \times 10^{-3} \text{ mm}^2/\text{s}$, respectively



leiomyomas. Leiomyomas showed variable SI on T2-weighted images, and may reflect a wide variety of histological features depending on degeneration or cellular content with abundant hyalinised collagen. The low ADC of ordinary leiomyomas can be explained by the “T2 blackout effect”, which indicates hypointensity on DWI caused by hypointensity on T2-weighted images [34, 35]. As DWI was

inherently T2-weighted imaging, changes in tissue T2 with SI near the background noise can influence the appearance of DWI independent of tissue diffusibility. Thus, we combined T2-weighted images to exclude ordinary leiomyomas with artificially lower ADC. Based on our results, myometrial tumours of high SI on T2-weighted images may be recommended for DWI. In previous studies, both

Fig. 2 A 55-year-old woman with hyperintense leiomyoma of the myometrium. **a** Axial T2-WI shows the well-defined myometrial mass as an area of heterogeneous high intensity. The TCR between the mass and the myometrium is 0.53 . **b** DWI on b_0 shows high signal intensity corresponding to the high intensity on the T2-weighted image of the leiomyoma. **c** DWI on $b_{1,000}$ visualises the mass as an area of hypointensity. When DWI on b_0 and $b_{1,000}$ are compared, a marked signal loss is detected on $b_{1,000}$ images. **d** ADC map demonstrates the tumour as an area of hyperintensity relative to the normal myometrium. The ADC values of leiomyoma and the normal myometrium are $1.65 \times 10^{-3} \text{ mm}^2/\text{s}$ and $1.15 \times 10^{-3} \text{ mm}^2/\text{s}$, respectively

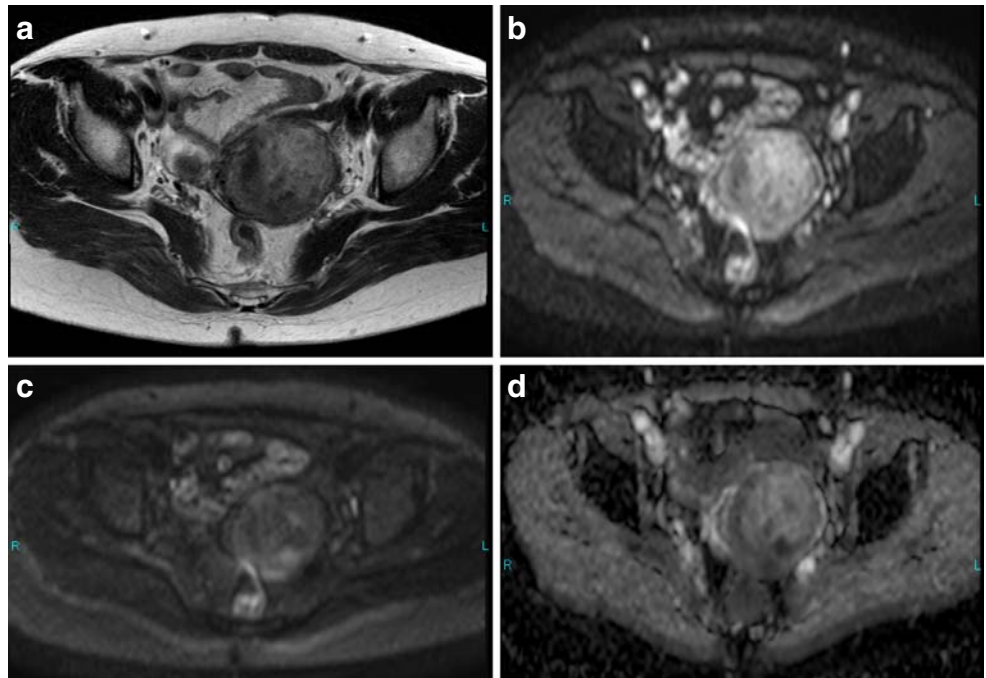
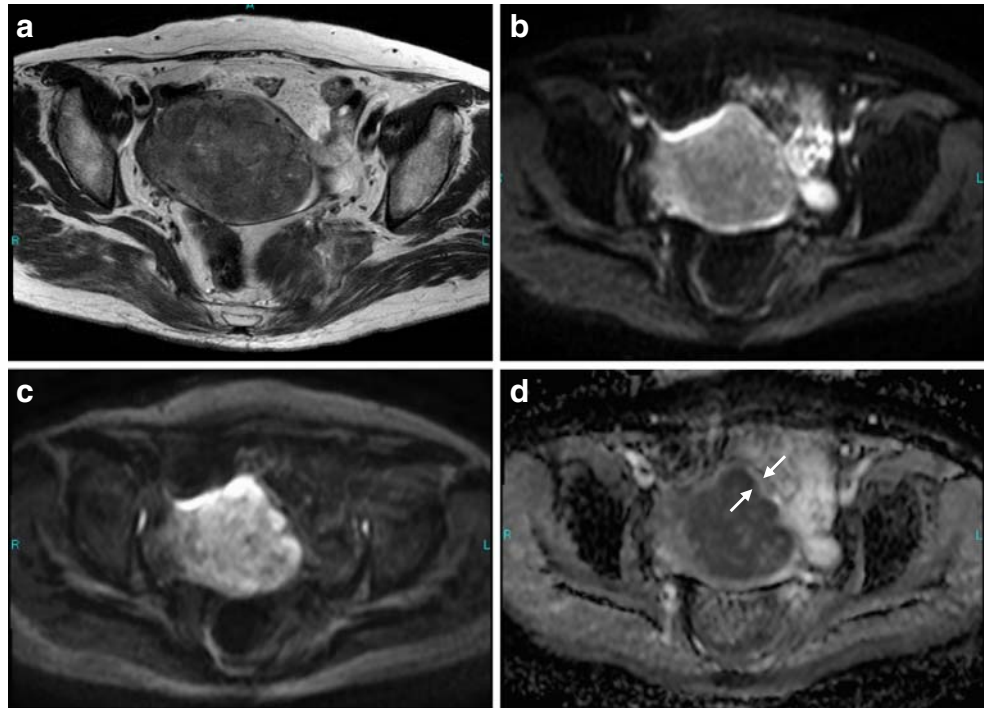


Fig. 3 A 58-year-old woman with leiomyosarcoma of the myometrium. **a** Axial T2-weighted image shows a myometrial mass of slightly high signal intensity invading the endometrial cavity. The TCR between the mass and the myometrium is 0.03. DWI on b_0 (**b**) and $b_{1,000}$ (**c**) demonstrating a hyperintense mass. When DWI on b_0 and $b_{1,000}$ are compared, a slight signal loss in the tumour is detected on the $b_{1,000}$ image. **d** ADC map demonstrates the tumour as an area of hypointensity and the normal myometrium as an area of hyperintensity (*arrows*). The ADC values of leiomyosarcoma and the normal myometrium are $0.95 \times 10^{-3} \text{ mm}^2/\text{s}$ and $1.57 \times 10^{-3} \text{ mm}^2/\text{s}$, respectively



degenerated and cellular leiomyomas exhibited hyperintensity on T2-weighted imaging [1, 5, 6, 12]. Tamai et al. [33] demonstrated that cellular leiomyomas may not be distinguished from sarcomas based on DWI and ADC values by increased cellularity. On the other hand, degenerated leiomyomas tended to exhibit low SI on DWI and higher ADC values compared with sarcomas. These results may

reflect the presence of abundant water content within the lesions. Accordingly, DWI and ADC measurement can aid in the differentiation between degenerated leiomyomas and sarcomas. Yamashita et al. [1] reported that slightly hyperintense tumours were more likely to be cellular leiomyoma, while markedly hyperintense tumours tended to be degenerated. Evaluation of TCR based on T2-

Fig. 4 A 27-year-old woman with endometrial stromal sarcoma of the myometrium. **a** Axial T2-weighted image shows a well-defined mass with high signal intensity in the myometrium. The TCR between the mass and the myometrium is 0.12. DWI on b_0 (**b**) and $b_{1,000}$ (**c**) demonstrating a hyperintense mass. When DWI on b_0 and $b_{1,000}$ are compared, a slight signal loss in the tumour is detected on the $b_{1,000}$ image. **d** ADC map demonstrates the tumour as an area of homogeneous hypointensity and the normal myometrium as an area of hyperintensity. The ADC values of the mass and the normal myometrium are $1.04 \times 10^{-3} \text{ mm}^2/\text{s}$ and $1.92 \times 10^{-3} \text{ mm}^2/\text{s}$, respectively

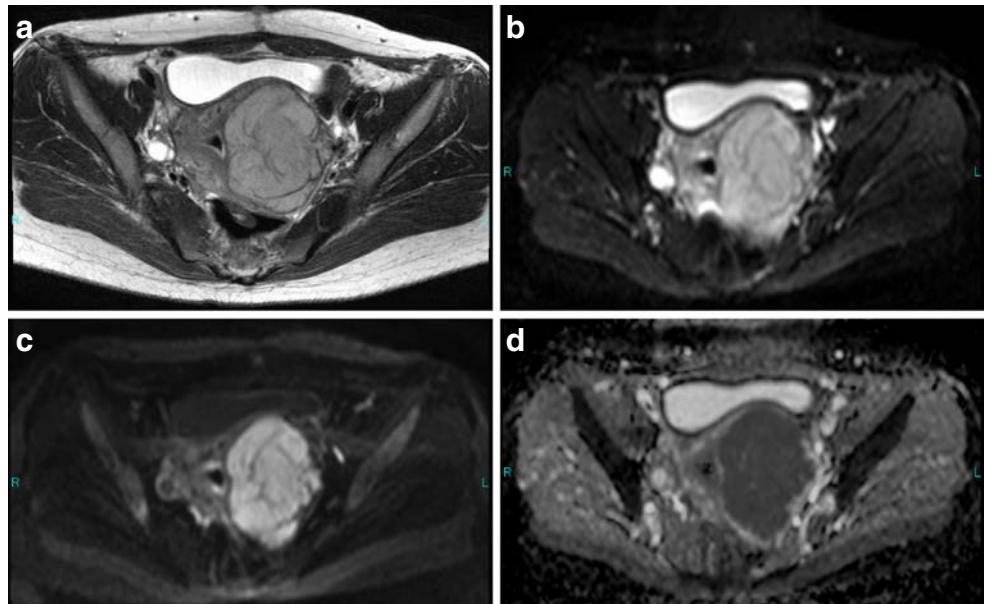


Fig. 5 A 57-year-old woman with endometrial mixed mesodermal tumours of the myometrium. **a** Axial T2-weighted image shows a myometrial mass of heterogeneous high signal intensity. The TCR between the mass and the myometrium is 0.37. DWI on b_0 (**b**) and $b_{1,000}$ (**c**) demonstrating a hyperintense mass. When DWI on b_0 and $b_{1,000}$ are compared, a slight signal loss in the tumour is detected on the $b_{1,000}$ image. **d** ADC map shows the tumour as an area of hypointensity and the normal myometrium as an area of hyperintensity. The ADC values of the mass and the normal myometrium are $0.74 \times 10^{-3} \text{ mm}^2/\text{s}$ and $1.40 \times 10^{-3} \text{ mm}^2/\text{s}$, respectively

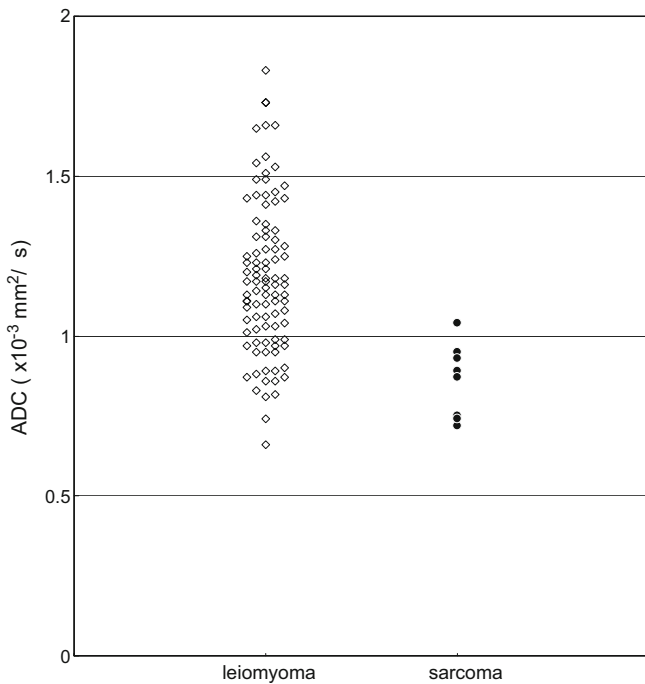
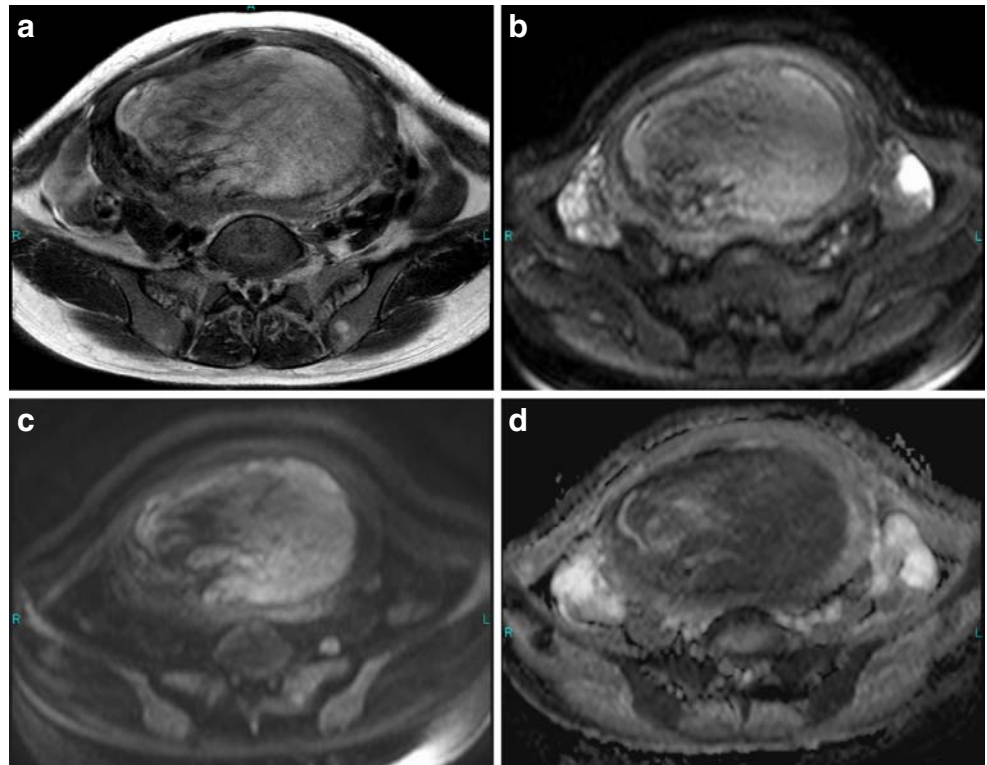


Fig. 6 Scatter plots of ADC values of leiomyomas and uterine sarcomas. Leiomyomas show significantly higher ADC values ($p < 0.01$) than uterine sarcomas. The ADC values overlap substantially for benign leiomyomas and uterine sarcomas

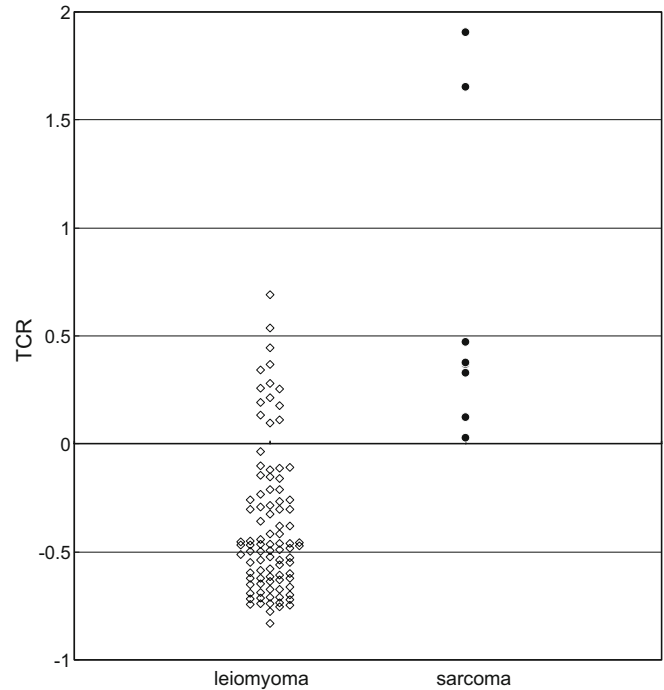


Fig. 7 Scatter plots of TCR of leiomyomas and uterine sarcomas. Leiomyomas show significantly lower TCR ($p < 0.01$) than those of uterine sarcomas. The TCR values between these two types of tumour show a considerable overlap

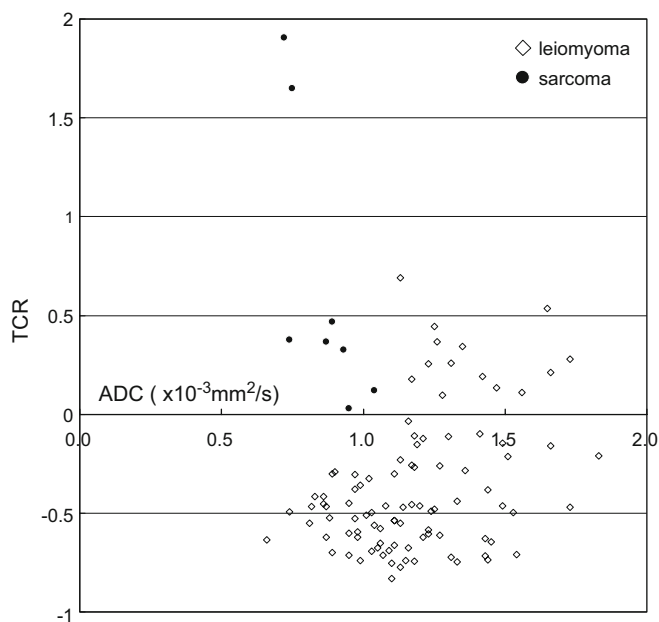


Fig. 8 Scatter plots of TCR versus ADC values of leiomyomas and uterine sarcomas. When ADC is less than $1.05 \times 10^{-3} \text{ mm}^2/\text{s}$ and TCR is greater than 0 this condition is considered to indicate a sarcoma; a combination of ADC and TCR avoids any overlap between sarcomas and leiomyomas

weighted imaging may be helpful in the differentiation between cellular and degenerative leiomyomas. However, we did not classify leiomyomas into histopathological subtypes, because some leiomyomas were not diagnostically proven. Thus, we may not have had cellular leiomyomas in this preliminary study.

In order to achieve images of diagnostic value, both high spatial resolution and high signal-to-noise ratio (SNR) are necessary to depict tissue characteristics. According to previous experience, the key problem of body DWI at 1.5 T is that the SNR is too low and ADC maps usually have too much noise [26–29]. Some previous studies have resolved this problem by using recently developed fusion software that can automatically overlay DWI onto ordinary MR images at 1.5 T [29, 33]. Therefore, DWI is only a supplement to T2-weighted imaging on 1.5-T systems. This perhaps is one of the reasons why uterine DWI has not been widely used on 1.5-T systems. Theoretically, the use of a higher magnetic field strength such as 3 T, with its related SNR gain, can enhance the performance of DWI and make it clinically feasible [36]. Greater radiofrequency power deposition and susceptibility effects than those of 1.5-T systems once limited the applicability of 3-T MR imaging, but the improvement of multichannel coils and the development of parallel imaging techniques have nearly overcome these problems. On the other hand, parallel imaging in virtually all other applications is

associated with an SNR penalty, which correlates with the degree of undersampling; the net SNR will be inversely proportional to the square root of the reduction factor. Accordingly, at a reduction factor of 2, parallel imaging will be associated with an SNR penalty of about 30–40%. A recent study suggested that MR imaging of the female pelvis at 3 T has the potential to provide excellent images of the uterine cervix and ovaries and equivalent images of the myometrium on high-resolution T2-weighted imaging at 1.5 T [37, 38]. However, to the best of our knowledge, the utility of DWI at 3 T compared with 1.5 T has not previously been investigated for body imaging. In comparison to 1.5 T, 3 T can provide faster acquisition times, higher SNR and greater spatial resolution. The increased SNR and improved spatial resolution at 3 T might result in the high performance of visual and quantitative analysis for myometrial lesions on DWI. To our knowledge, this will be the first published study to calculate ADC maps from the DWI of the female pelvis on a 3-T MR unit. The mean ADC values for the normal myometrium in the present study at 3 T and the previous study at 1.5 T were $1.58 \pm 0.22 \times 10^{-3} \text{ mm}^2/\text{s}$ and $1.62 \pm 0.11 \times 10^{-3} \text{ mm}^2/\text{s}$ [33], respectively. The mean ADC values of the normal endometrium at 3 T were similar to those previously determined at 1.5 T. The absence of a large difference in ADC between 1.5 T and 3 T was in agreement with the fact that the ADC values at 3 T were reliable.

There are some limitations to our study. First, the number of uterine sarcomas was relatively small, although malignant and benign tumours had significantly different ADC values. Thus, a larger study should be prospectively performed to verify our results. Second, some leiomyomas were not diagnostically proven: typical clinical and laboratory findings, in combination with follow-up imaging findings, were used as diagnostic criteria for these patients. Thus, we did not classify leiomyomas into histopathological subtypes. Third, our study population does not include patients with other benign myometrial conditions, such as adenomyosis. Therefore, the ability of ADC values to differentiate between malignant and non-malignant myometrial lesions, except for leiomyomas, is uncertain.

Conclusion

DWI is feasible for demonstrating uterine myometrial tumours on 3-T MR imaging. The ADC values of uterine sarcomas are significantly lower than those of leiomyomas, although the differentiation between uterine sarcomas and leiomyomas based on ADC values alone seems difficult because of a large overlap. Our preliminary results indicate that the combination of ADC and TCR based on T2-weighted imaging is significantly better than ADC or T2-weighted imaging alone at differentiating between sarcomas and leiomyomas.

References

1. Yamashita Y, Torashima M, Takahashi M, Tanaka N, Katabuchi H, Miyazaki K, Ito M, Okamura H (1993) Hyperintense uterine leiomyoma at T2-weighted MR imaging: differentiation with dynamic enhanced MR imaging and clinical implications. *Radiology* 189:721–725
2. Spies JB, Roth AR, Jha RC, Gomez-Jorge J, Levy EB, Chang TC, Ascher SA (2002) Leiomyomata treated with uterine artery embolization: factors associated with successful symptom and imaging outcome. *Radiology* 222:45–52
3. Smart OC, Hindley JT, Regan L, Gedroyc WM (2006) Magnetic resonance guided focused ultrasound surgery of uterine fibroids—the tissue effects of GnRH agonist pre-treatment. *Eur J Radiol* 59:163–167
4. Sahdev A, Sohaib SA, Jacobs I, Shepherd JH, Oram DH, Reznick RH (2001) MR imaging of uterine sarcomas. *AJR Am J Roentgenol* 177:1307–1311
5. Goto A, Takeuchi S, Sugimura K, Maruo T (2002) Usefulness of Gd-DTPA contrast-enhanced dynamic MRI and serum determination of LDH and its isozymes in the differential diagnosis of leiomyosarcoma from degenerated leiomyoma of the uterus. *Int J Gynecol Cancer* 12:354–361
6. Tanaka Y, Nishida M, Tsunoda H, Okamoto Y, Yoshikawa H (2004) Smooth muscle tumors of uncertain malignant potential and leiomyosarcomas of the uterus: MR findings. *J Magn Reson Imaging* 20:998–1007
7. Koyama T, Togashi K, Konishi I, Kobayashi H, Ueda H, Kataoka ML, Itoh T, Higuchi T, Fujii S, Konishi J (1999) MR imaging of endometrial stromal sarcoma: correlation with pathologic findings. *AJR Am J Roentgenol* 173:767–772
8. Ueda M, Otsuka M, Hatakenaka M, Torii Y (2000) Uterine endometrial stromal sarcoma located in uterine myometrium: MRI appearance. *Eur Radiol* 10:780–782
9. Ueda M, Otsuka M, Hatakenaka M, Sakai S, Ono M, Yoshimitsu K, Honda H, Torii Y (2001) MR imaging findings of uterine endometrial stromal sarcoma: differentiation from endometrial carcinoma. *Eur Radiol* 11:28–33
10. Togashi K, Ozasa H, Konishi I, Itoh H, Nishimura K, Fujisawa I, Noma S, Sagoh T, Minami S, Yamashita K et al (1989) Enlarged uterus: differentiation between adenomyosis and leiomyoma with MR imaging. *Radiology* 171:531–534
11. Hricak H, Tscholakoff D, Heinrichs L, Fisher MR, Doooms GC, Reinhold C, Jaffe RB (1986) Uterine leiomyomas: correlation of MR, histopathologic findings, and symptoms. *Radiology* 158:385–391
12. Ueda H, Togashi K, Konishi I, Kataoka ML, Koyama T, Fujiwara T, Kobayashi H, Fujii S, Konishi J (1999) Unusual appearances of uterine leiomyomas: MR imaging findings and their histopathologic backgrounds. *Radiographics* 19:S131–S145
13. Le Bihan D, Breton E, Lallemand D, Grenier P, Cabanis E, Laval-Jeantet M (1986) MR imaging of intravoxel incoherent motions: application to diffusion and perfusion in neurologic disorders. *Radiology* 161:401–407
14. Li TQ, Takahashi AM, Hindmarsh T, Moseley ME (1999) ADC mapping by means of a single-shot spiral MRI technique with application in acute cerebral ischemia. *Magn Reson Med* 41:143–147
15. Schaefer PW, Grant PE, Gonzalez RG (2000) Diffusion-weighted MR imaging of the brain. *Radiology* 217:331–345
16. Kurihara Y, Yakushiji YK, Tani I, Nakajima Y, Van Cauteren M (2002) Coil sensitivity encoding in MR imaging: advantages and disadvantages in clinical practice. *AJR Am J Roentgenol* 178:1087–1091
17. Namimoto T, Yamashita Y, Sumi S, Tang Y, Takahashi M (1997) Focal liver masses: characterization with diffusion-weighted echo-planar MR imaging. *Radiology* 204:739–744
18. Yamashita Y, Tang Y, Takahashi M (1998) Ultrafast MR imaging of the abdomen: echo planar imaging and diffusion-weighted imaging. *J Magn Reson Imaging* 8:367–374
19. Sato C, Naganawa S, Nakamura T, Kumada H, Miura S, Takizawa O, Ishigaki T (2005) Differentiation of noncancerous tissue and cancer lesions by apparent diffusion coefficient values in transition and peripheral zones of the prostate. *J Magn Reson Imaging* 21:258–262
20. Charles-Edwards EM, deSouza NM (2006) Diffusion-weighted magnetic resonance imaging and its application to cancer. *Cancer Imaging* 13; 6:135–143
21. Koyama T, Tamai K, Togashi K (2006) Current status of body MR imaging: fast MR imaging and diffusion-weighted imaging. *Int J Clin Oncol* 11:278–285
22. Szafer A, Zhong J, Gore JC (1995) Theoretical model for water diffusion in tissues. *Magn Reson Med* 33:697–712
23. Liu KF, Li F, Tatlisumak T, Garcia JH, Sotak CH, Fisher M, Fenstermacher JD (2001) Regional variations in the apparent diffusion coefficient and the intracellular distribution of water in rat brain during acute focal ischemia. *Stroke* 32:1897–1905
24. Knight RA, Ordidge R, Helpert J, Chopp M, Rodolosi L, Peck D (1991) Temporal evolution of ischemic damage in rat brain measured by proton nuclear magnetic resonance imaging. *Stroke* 22:802–808
25. Matoba M, Tonami H, Kondou T, Yokota H, Higashi K, Toga H, Sakuma T (2007) Lung carcinoma: diffusion-weighted MR imaging—preliminary evaluation with apparent diffusion coefficient. *Radiology* 243:570–577
26. Moteki T, Ishizaka H (2000) Diffusion-weighted EPI of cystic ovarian lesions: evaluation of cystic contents using apparent diffusion coefficients. *J Magn Reson Imaging* 12:1014–1019
27. Nakayama T, Yoshimitsu K, Irie H, Aibe H, Tajima T, Nishie A, Asayama Y, Matak K, Kakiyama D, Matsuura S, Nakano H, Honda H (2005) Diffusion-weighted echo-planar MR imaging and ADC mapping in the differential diagnosis of ovarian cystic masses: usefulness of detecting keratinoid substances in mature cystic teratomas. *J Magn Reson Imaging* 22:271–278
28. Naganawa S, Sato C, Kumada H, Ishigaki T, Miura S, Takizawa O (2005) Apparent diffusion coefficient in cervical cancer of the uterus: comparison with the normal uterine cervix. *Eur Radiol* 15:71–78
29. Tamai K, Koyama T, Saga T, Umeoka S, Mikami Y, Fujii S, Togashi K (2007) Diffusion-weighted MR imaging of uterine endometrial cancer. *J Magn Reson Imaging* 26:682–687
30. Jacobs MA, Herskovits EH, Kim HS (2005) Uterine fibroids: diffusion weighted MR imaging for monitoring therapy with focused ultrasound surgery—preliminary study. *Radiology* 236:196–203

31. Liapi E, Kamel IR, Bluemke DA, Jacobs MA, Kim HS (2005) Assessment of response of uterine fibroids and myometrium to embolization using diffusion-weighted echoplanar MR imaging. *J Comput Assist Tomogr* 29:83–86
32. Shimada K, Ohashi I, Kasahara I, Watanabe H, Ohta S, Miyasaka N, Itoh E, Shibuya H (2004) Differentiation between completely hyalinized uterine leiomyomas and ordinary leiomyomas: three-phase dynamic magnetic resonance imaging (MRI) vs diffusion weighted MRI with very small b-factors. *J Magn Reson Imaging* 20:97–104
33. Tamai K, Koyama T, Saga T, Morisawa N, Fujimoto K, Mikami Y, Togashi K (2008) The utility of diffusion-weighted MR imaging for differentiating uterine sarcomas from benign leiomyomas. *Eur Radiol* 18:723–730
34. Maldjian JA, Listerud J, Moonis G, Siddiqi F (2001) Computing diffusion rates in T2-dark hematomas and areas of low T2 signal. *AJNR Am J Neuroradiol* 22:112–118
35. Silvera S, Oppenheim C, Touzé E, Ducreux D, Page P, Domigo V, Mas JL, Roux FX, Frédy D, Meder JF (2005) Spontaneous intracerebral hematoma on diffusion-weighted images: influence of T2-shine-through and T2-blackout effects. *AJNR Am J Neuroradiol* 26:236–241
36. Lee VS, Hecht EM, Taouli B, Chen Q, Prince K, Oesingmann N (2007) Body and cardiovascular MR imaging at 3.0 T. *Radiology* 244:692–705
37. Morakkabati-Spitz N, Schild HH, Kuhl CK, Lutterbey G, von Falkenhausen M, Träber F, Gieseke J (2006) Female pelvis: MR imaging at 3.0 T with sensitivity encoding and flip-angle sweep technique. *Radiology* 241:538–545
38. Kataoka M, Kido A, Koyama T, Isoda H, Umeoka S, Tamai K, Nakamoto Y, Maetani Y, Morisawa N, Saga T, Togashi K (2007) MRI of the female pelvis at 3T compared to 1.5T: evaluation on high-resolution T2-weighted and HASTE images. *J Magn Reson Imaging* 25:527–534